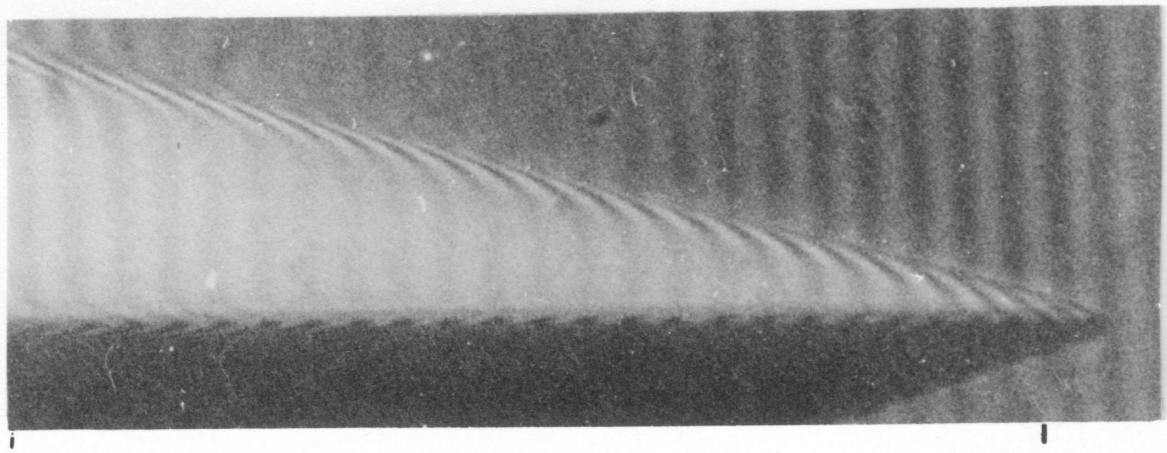

0 1 cm

Wedge angle = 41°
Time from shock reflection = 200 μsec
Nozzle stagnation condition = B2

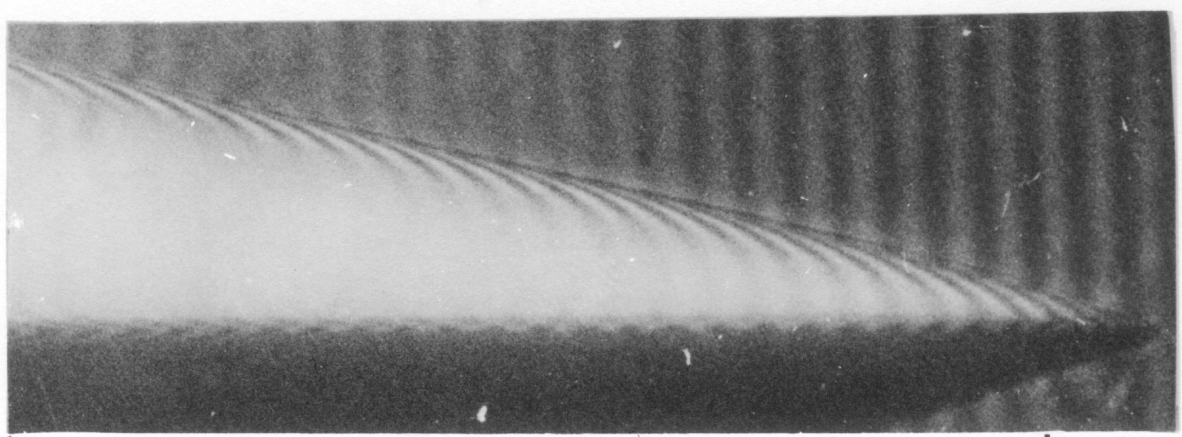

0 1 cm

Wedge angle = 41°
Time from shock reflection = 200 μsec
Nozzle stagnation condition = B3

Fringe contours of .1

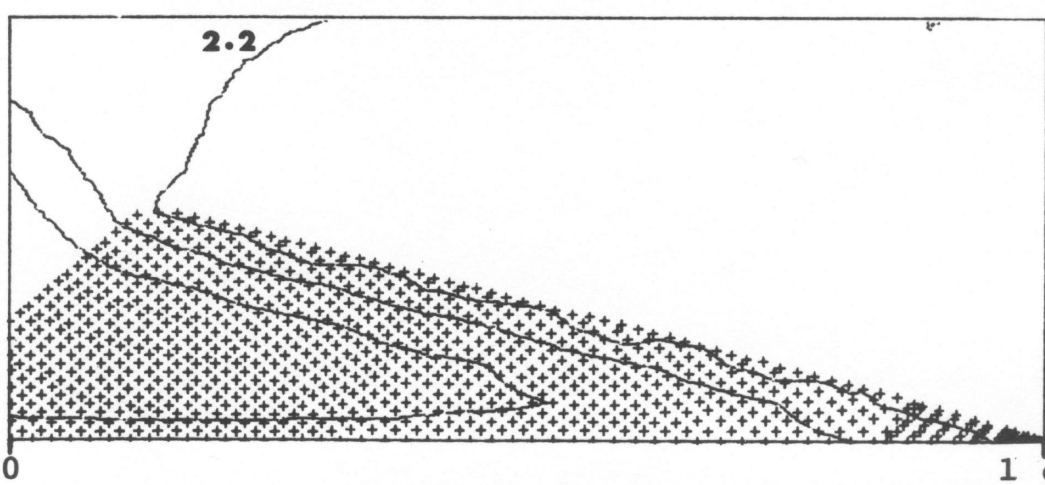

Figure 3.12: Two interferograms of flow over a wedge and a calculated flow field.

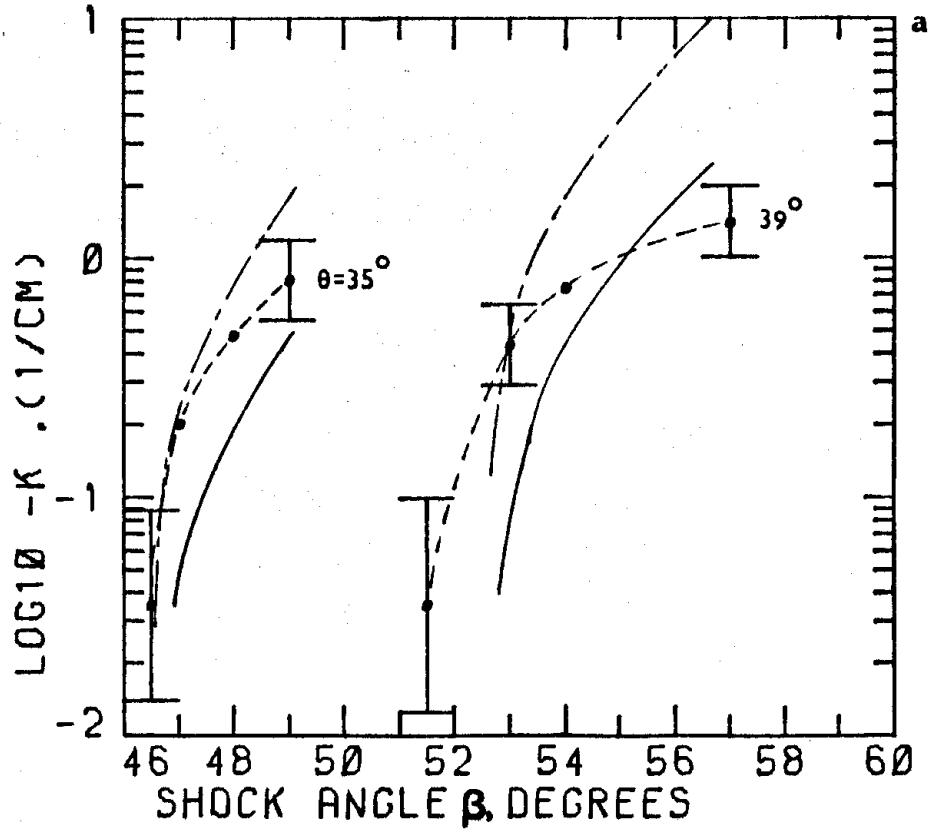

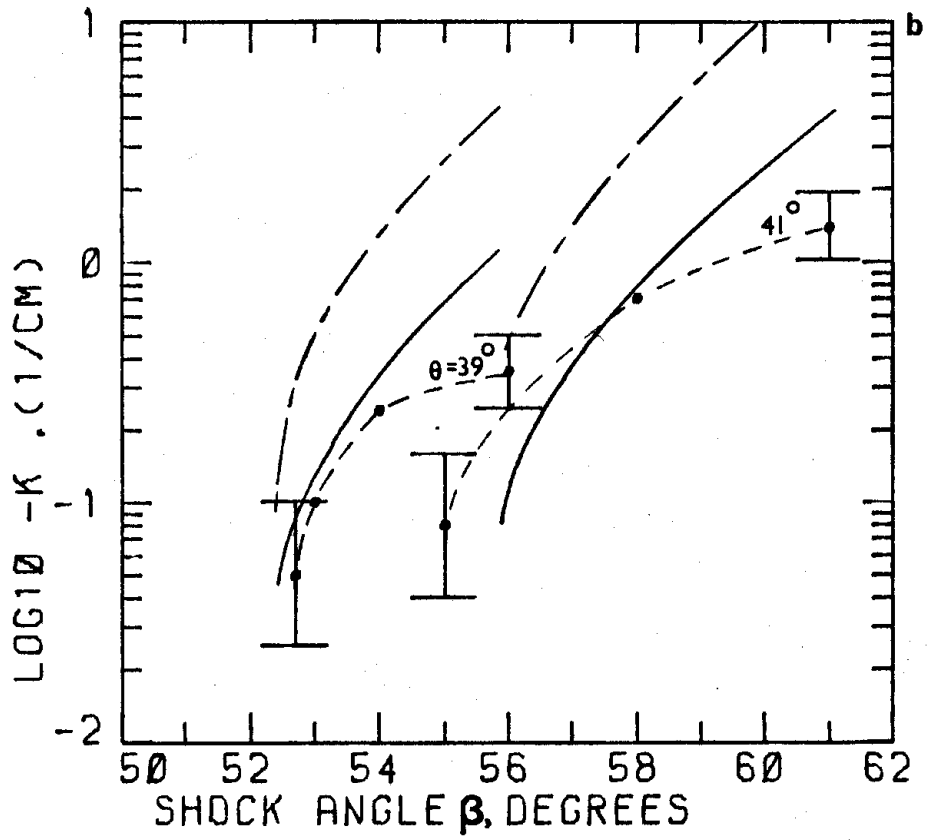

Figures 3.13a and b: Comparison of experimental and theoretical shock curvature due to vibrational relaxation. – · – · – , experimental; ——, calculated with the value of τ_v given by Millikan and White (1963a) and Appleton (1967); —— – ——, calculated with $\tau_v/4$.

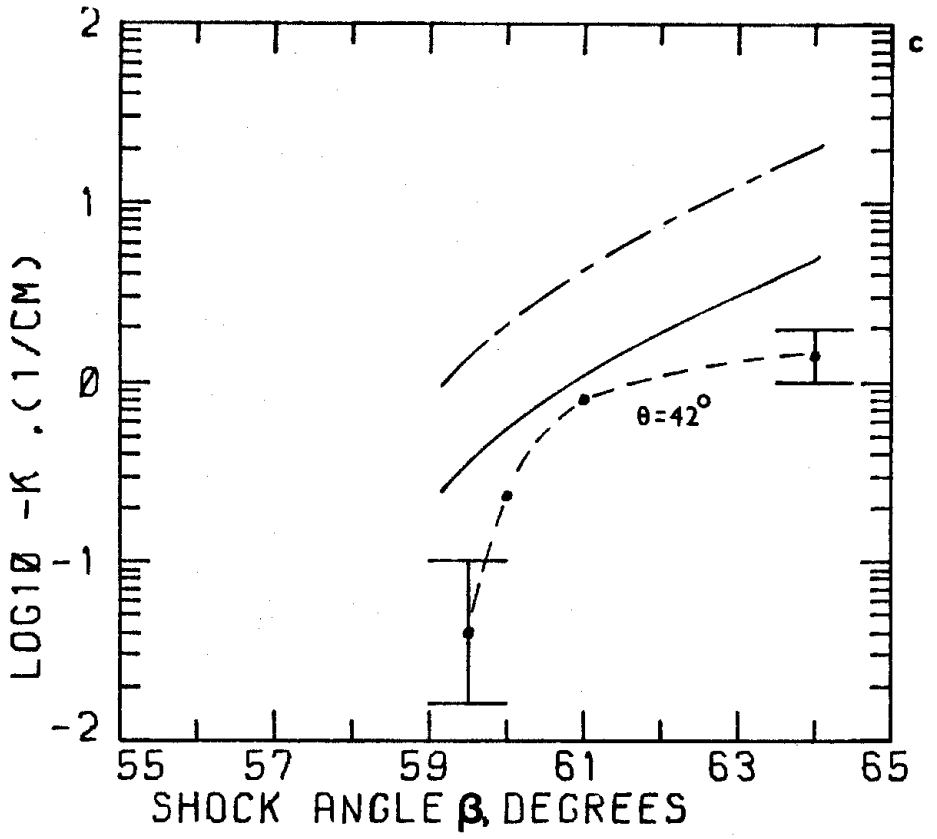

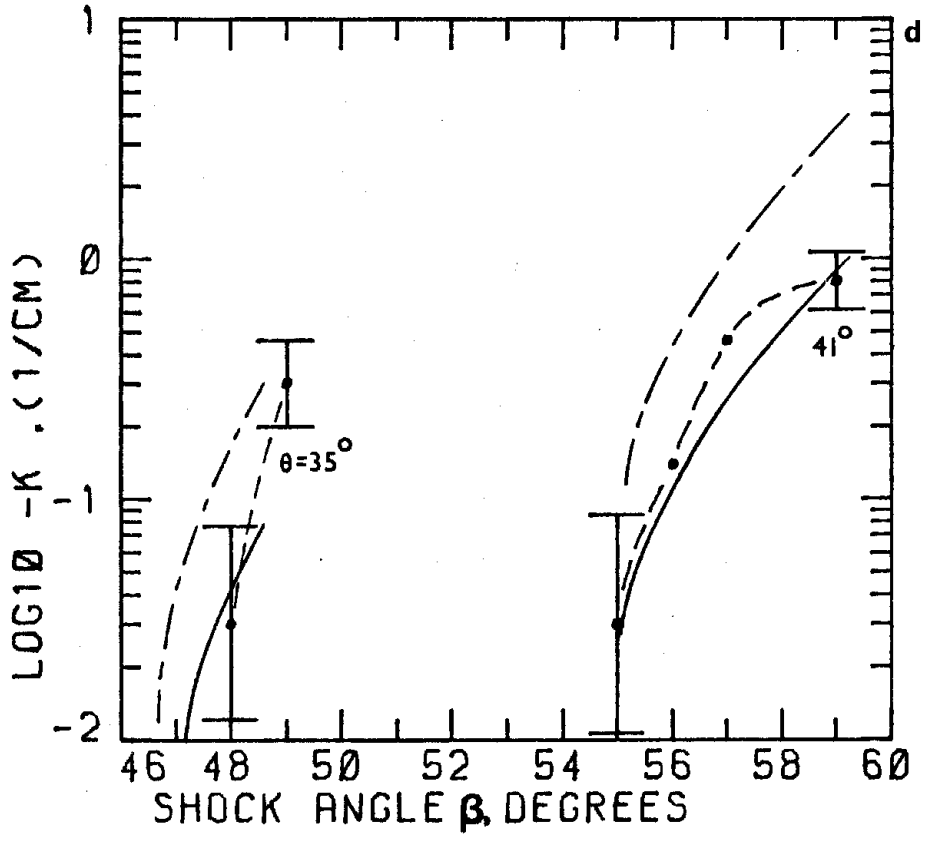

Figures 3.13c and d: Comparison of experimental and theoretical shock curvature due to vibrational relaxation. For the legend see Figures 3.13a and b. The free-stream conditions for a, b, c and d correspond to the cases A5, B2, C1 and B3 given in Table 3.1.

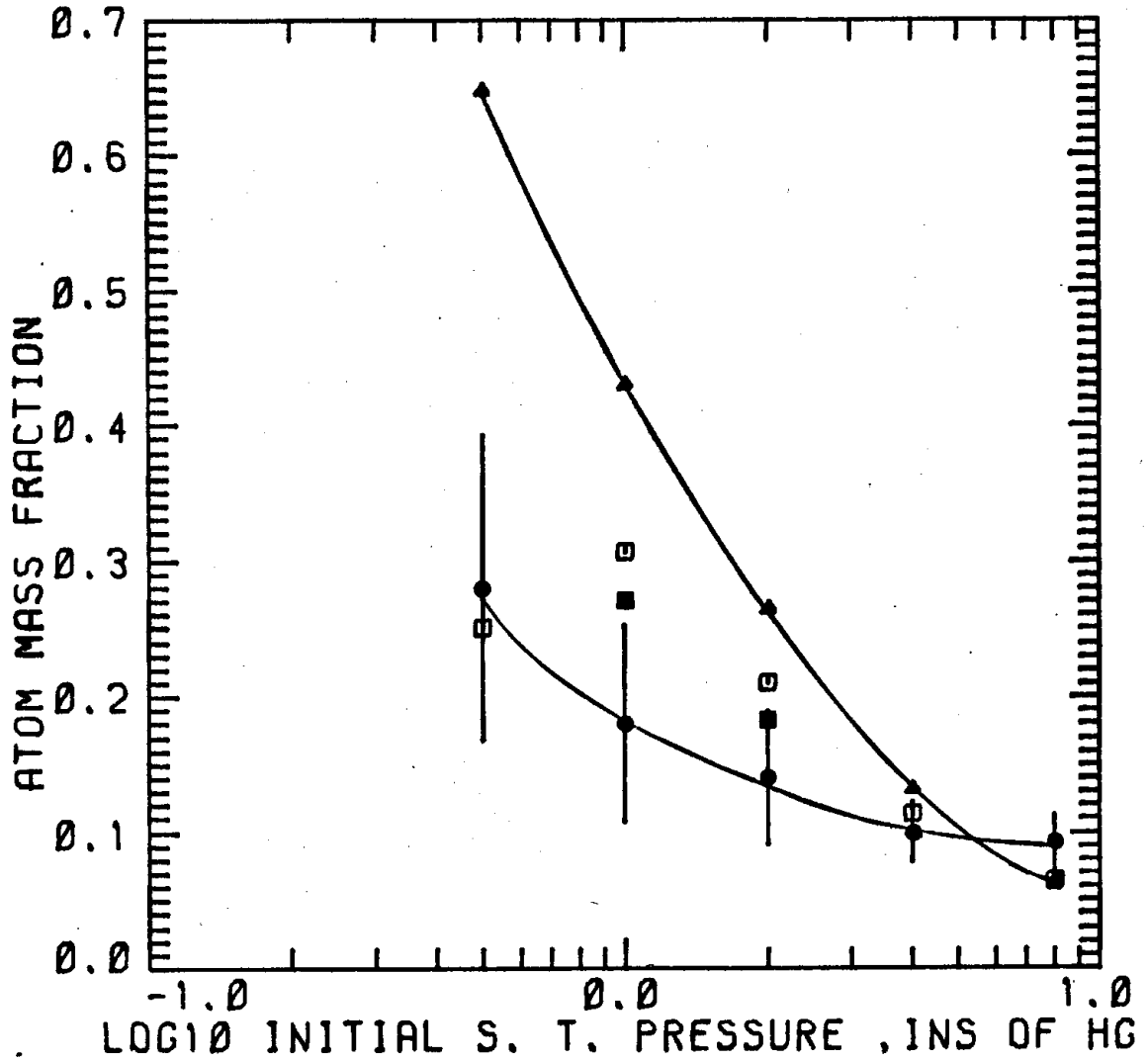

Figure 3.14: Comparison of measured and predicted atom mass fraction of nitrogen in T3 versus initial shock tube pressure (p_1). ● , experimental results from Crane (1975). ▲ , predicted with no He contamination; ⊡ , predicted with He contamination given by Crane (1975); ■ , predicted with expected maximum He contamination. The rates of Appleton et al. (1968) are used in the calculations. The stagnation conditions are given in the following table.

p_1, in. of Hg	8	4	2	1	½
P_o, atm	270	280	300	265	230
T_o, K (no He)	8900	9670	11100	11800	14160
T_o, K(He)	8900	9500	10375	10950	10750
r, (see text)	0	0.09±35%	0.20±55%	0.38±55%	1.9±80%

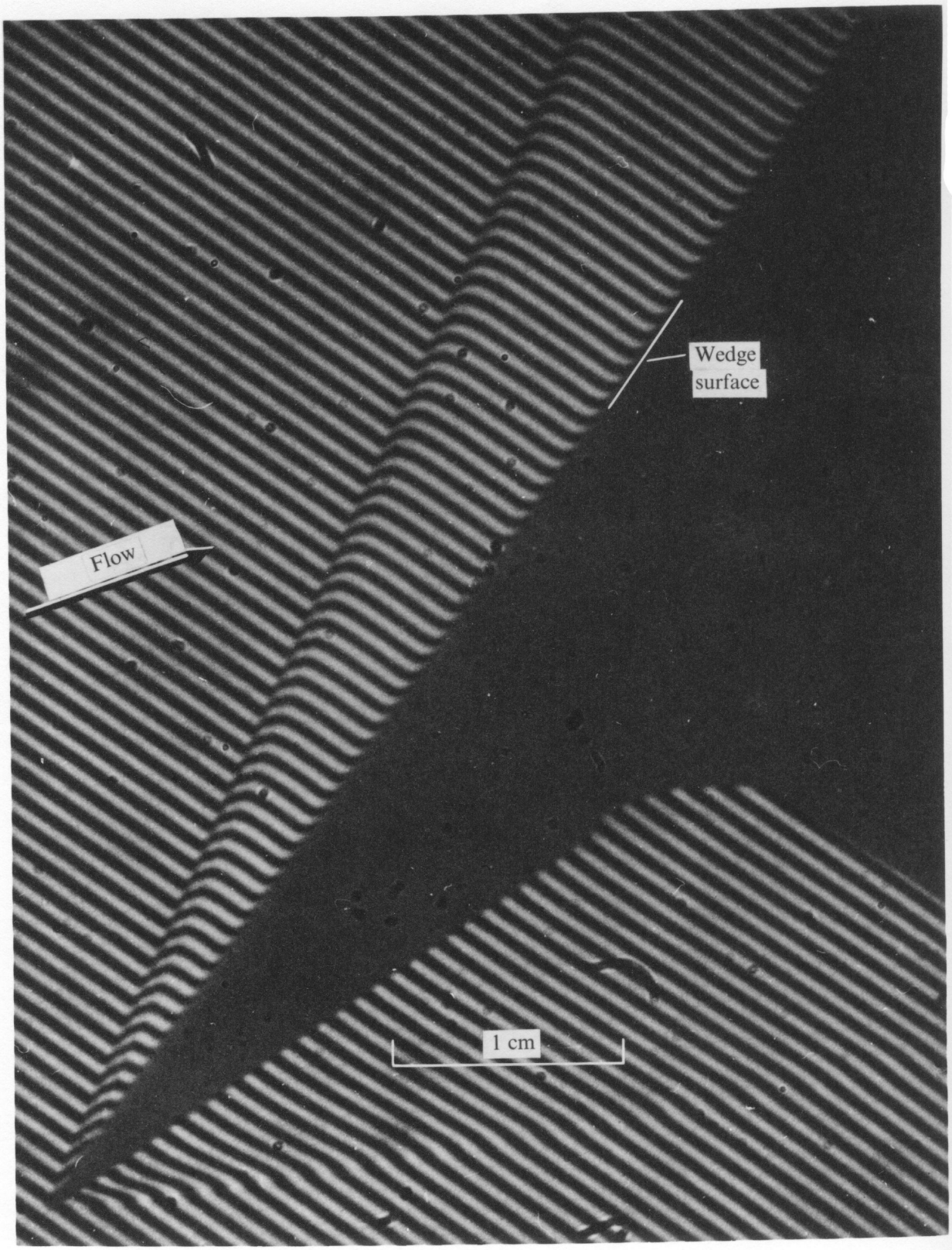

Figure 3.15: Interferogram of flow over a flat plate at 35° incidence. The initial shock tube pressure is 6" of Hg of N_2.

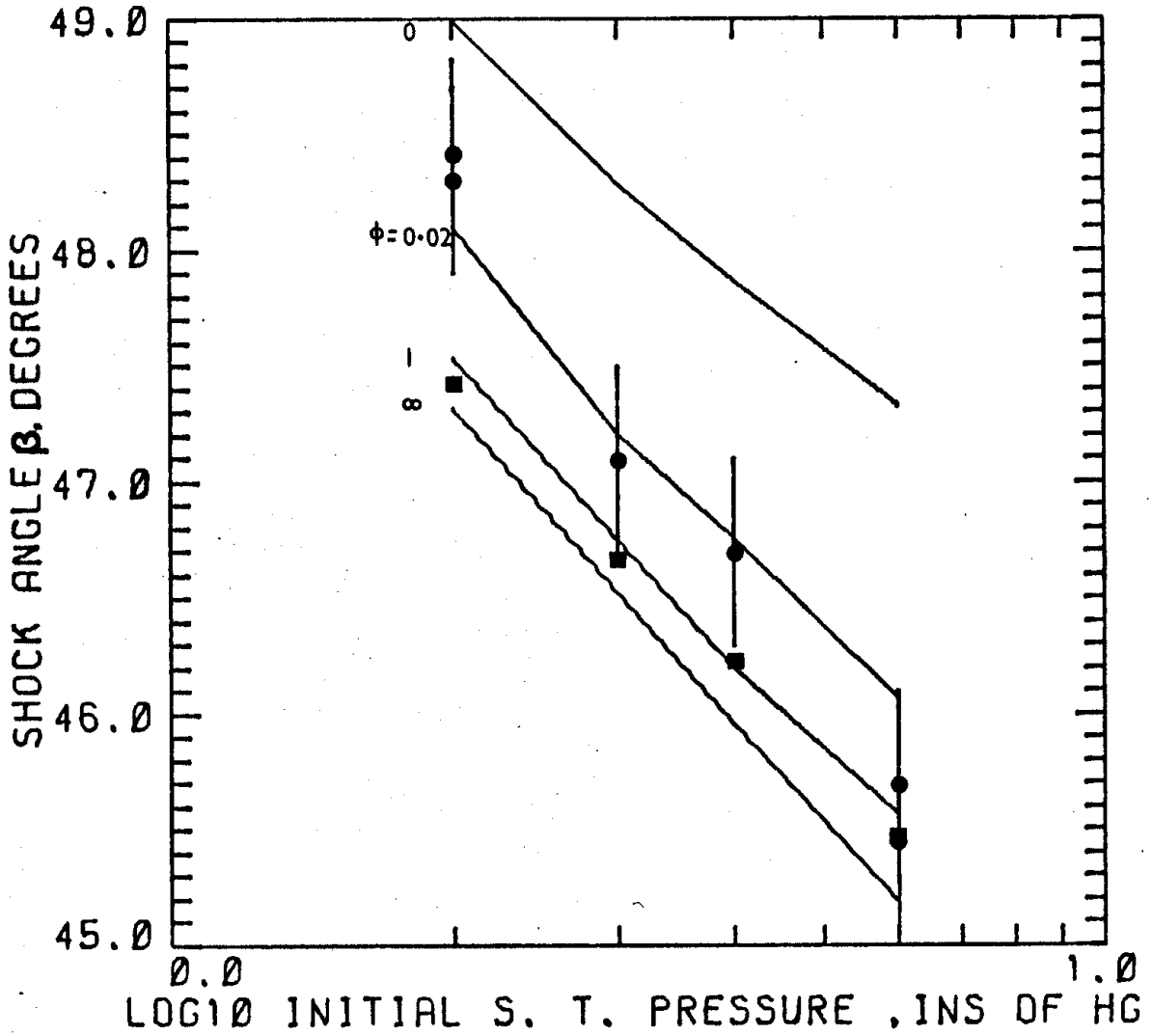

Figure 3.16: Calculated and measured shock angle on a 35° wedge in T3 versus initial shock tube pressure of nitrogen. ϕ represents the ratio of vibrational de-excitation rate to excitation rate used in the nozzle flow calculations. ● , experiment; ——— , calculated with no He contamination; ■ , calculated with He contamination (ϕ = 1).

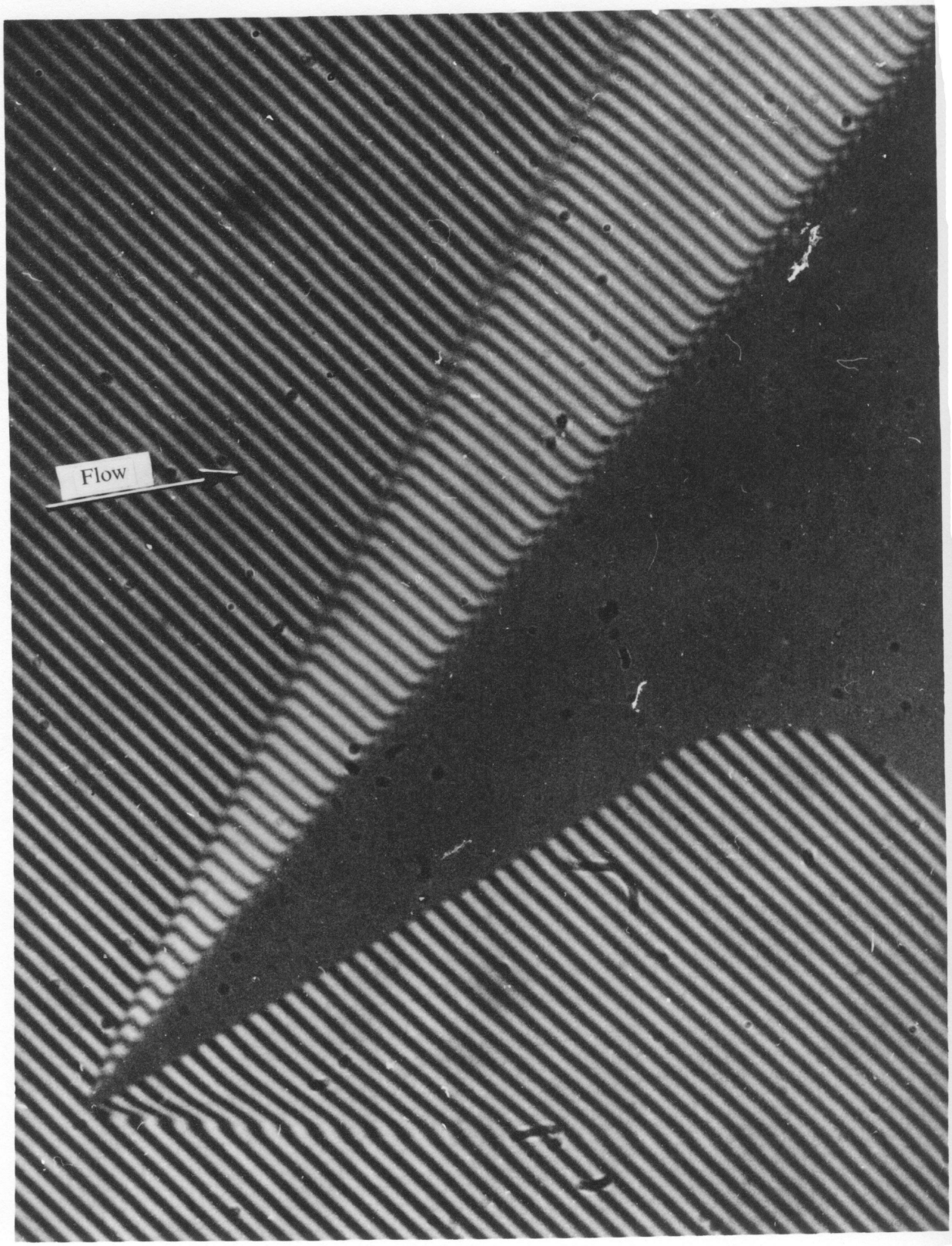

Figure 3.17: Interferogram of flow over a flat plate at 41.5° incidence. The initial shock tube pressure is 6" of Hg of N_2.

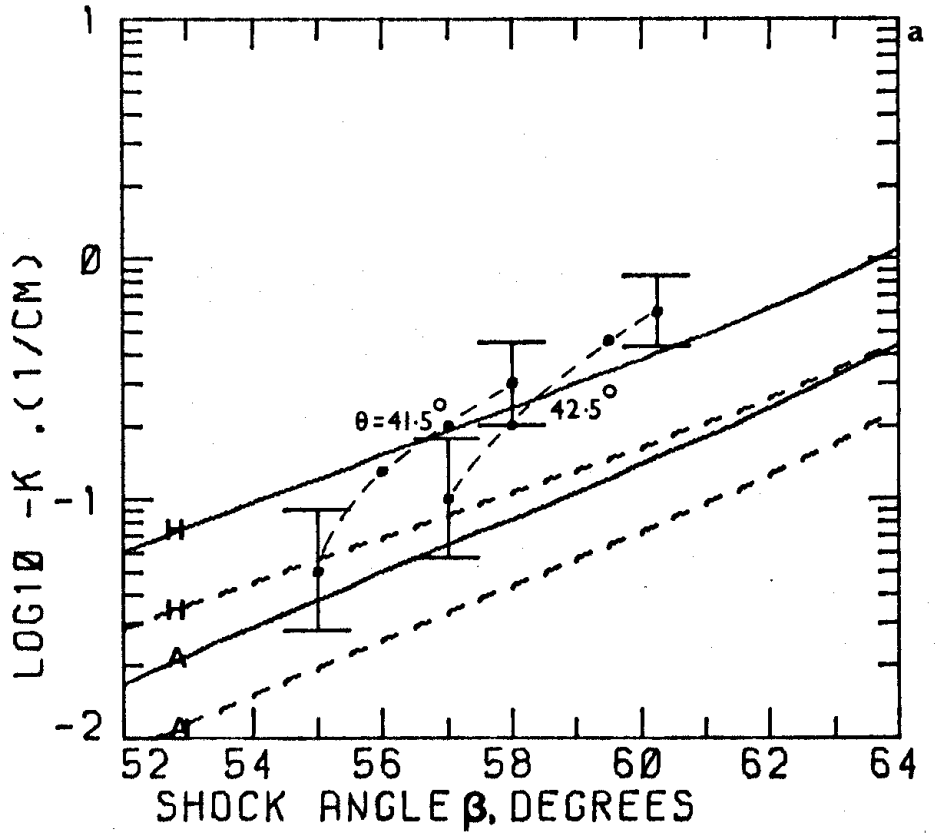

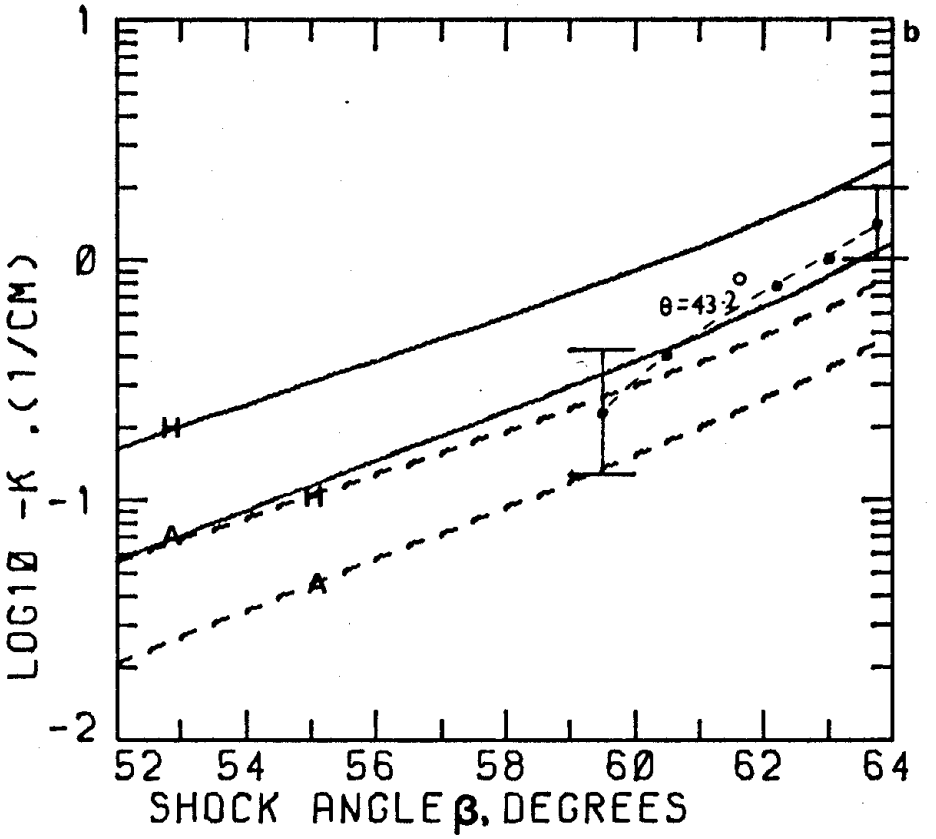

Figures 3.18a and b: Comparison of experimental shock curvature and predicted initial shock curvature due to dissociation. ---•--- , experimental; —A— , predicted with the rates of Appleton et al. (1968); —H—, predicted with the rates of Hanson and Baganoff (1972); both predictions with no helium contamination. Predictions with helium contamination are denoted by - - -. Note that for agreement between experiment and theory, the right-hand end of the experimental curve should fall on the theoretical curve.

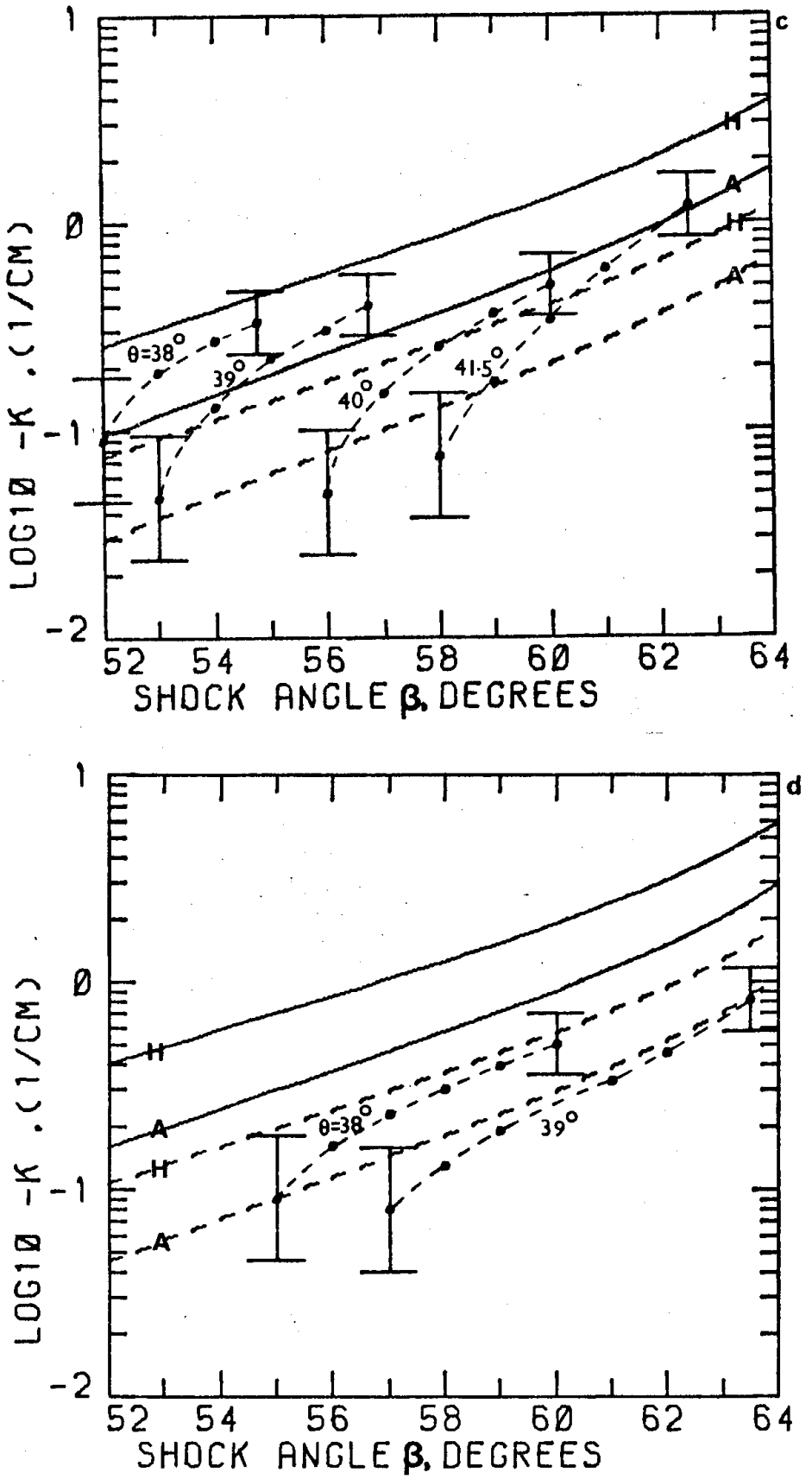

Figures 3.18c and d: Comparison of experimental shock curvature and predicted initial shock curvature due to dissociation. For the legend see Figures 3.18a and b. The free-stream conditions for a,b,c and d correspond to the cases I, II, III and IV given in Table 3.2.

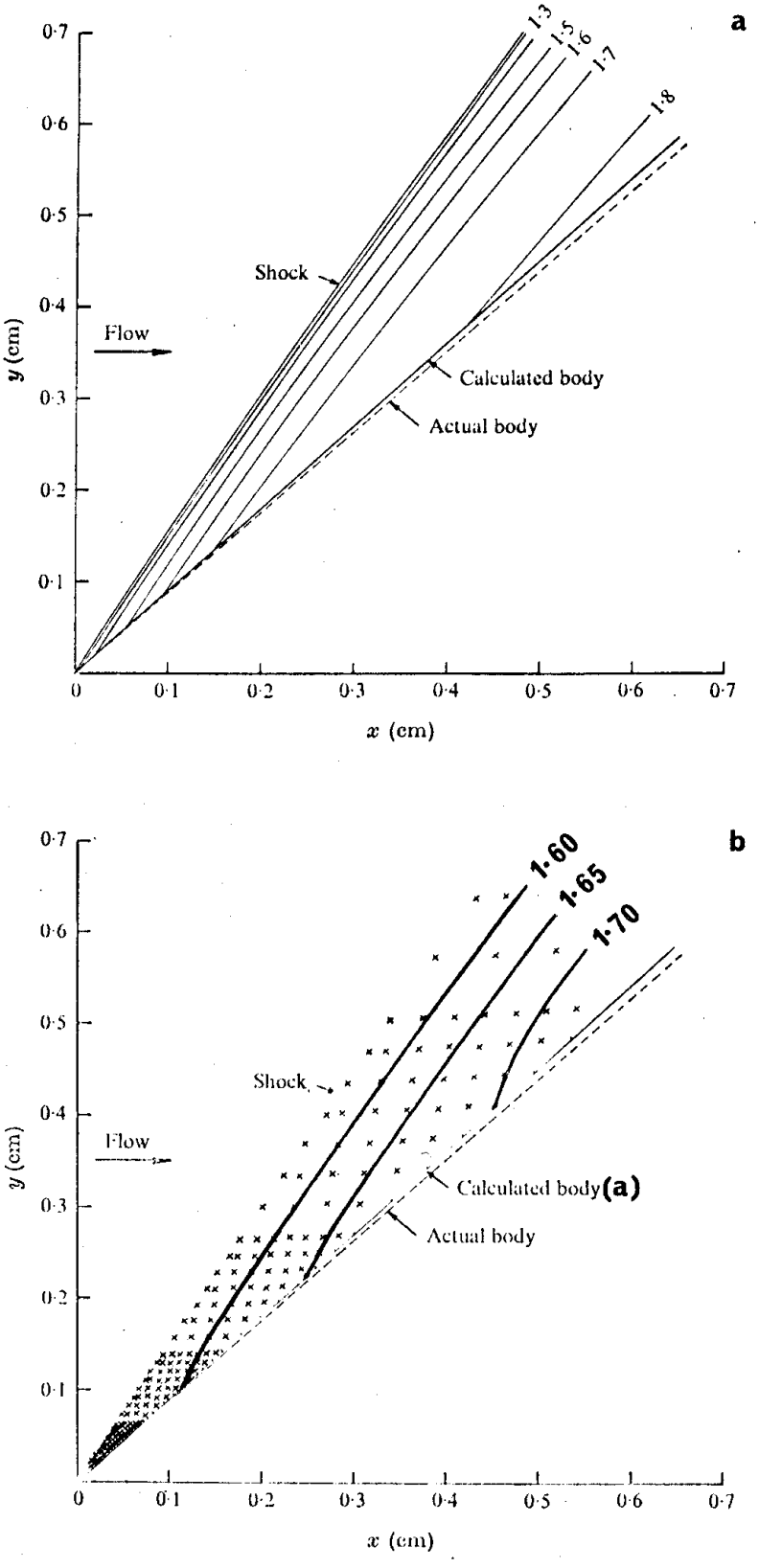

Figure 3.19: Flow field calculated by the inverse method and the method of characteristics using the reaction rates of section 3.2.

(a) The inverse method, starting from the measured shock shape of Figure 3.17, gives a calculated body slope of 42.2°. The actual plate incidence is 41.5°.

(b) The method of characteristics calculation starts from the body slope of 42.2°.

The curves represent contours of fringe shift, the value of which, relative to the free-stream, is indicated by the numbers.

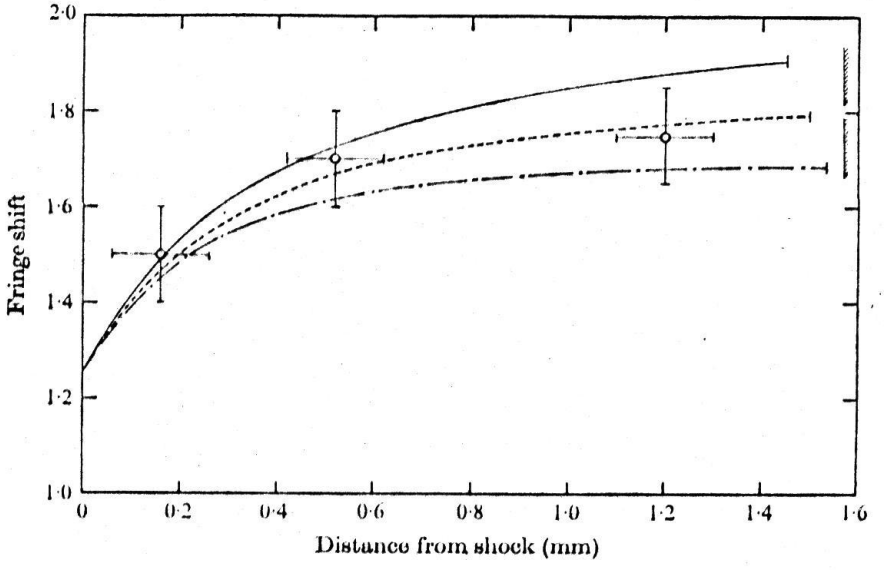

Figure 3.20: Profile of fringe shift across the shock layer at 0.6cm from the tip of the wedge at conditions corresponding to Figure 3.17. o , experiment; — - —, calculated with the rates of Appleton et al. (1968); ————, calculated with the rates of Hanson and Baganoff (1972); ---, calculated with the rates of section 3.2. The curves are terminated at the predicted body point. ||||||||| indicates the actual body position.

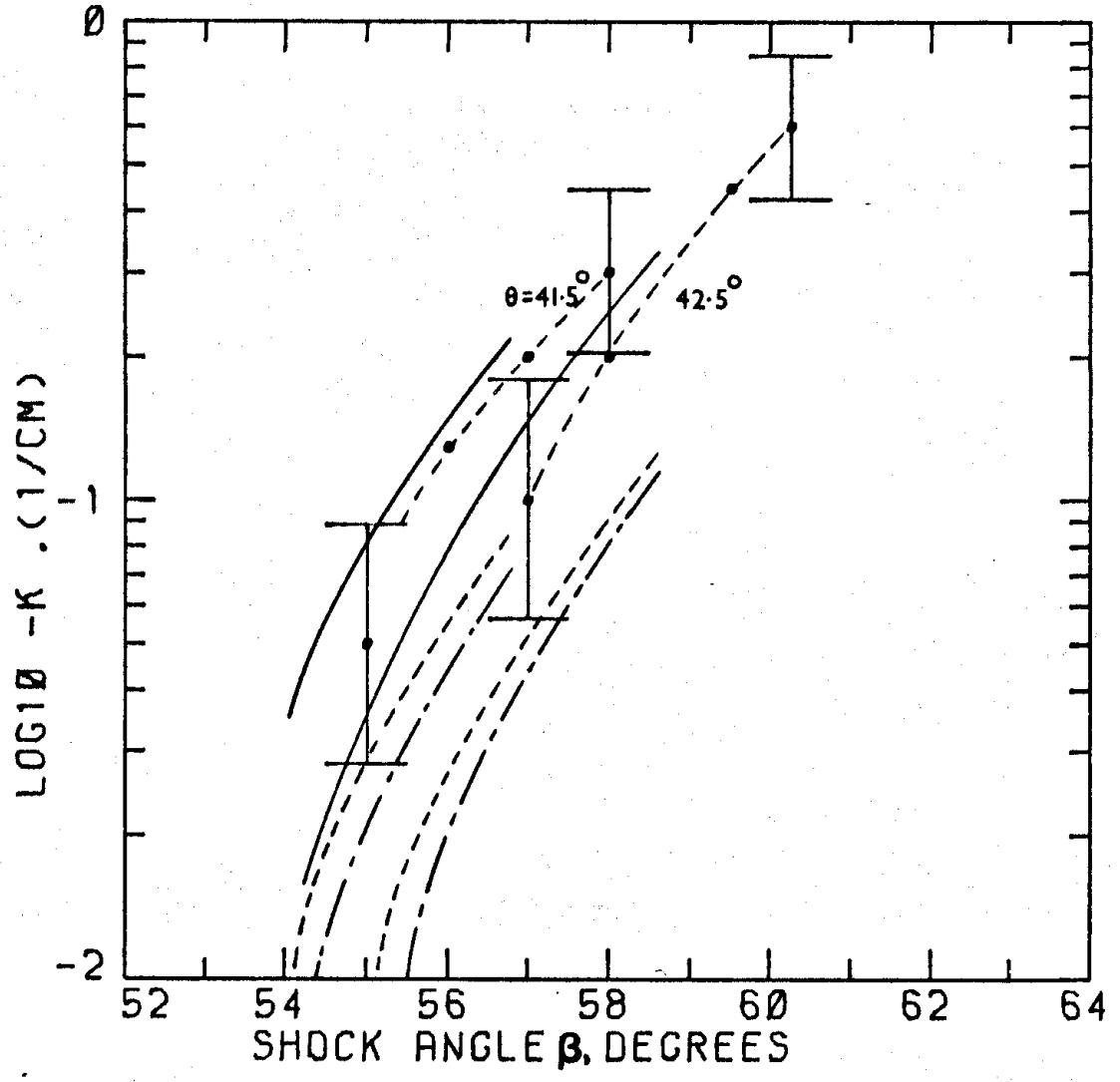

Figure 3.21: Comparison of experimental and theoretical shock curvature due to dissociation. The free-stream conditions correspond to case I. —·—·— , experiment; — - —, calculated with the rates of Appleton et al. (1968); ————, calculated with the rates of Hanson and Baganoff (1972); ---, calculated with the rates of section 3.2.